

Synthesis and Characterization of a Fluorescent Analogue of Cyclic di-GMP

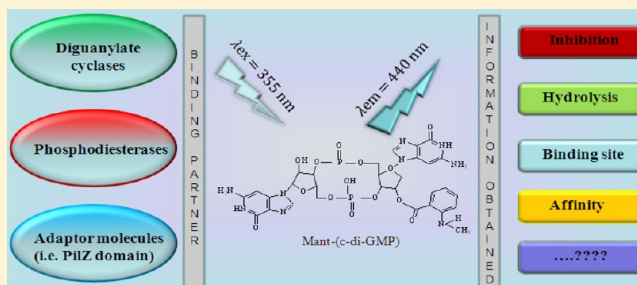
Indra Mani Sharma,[†] Thillaivillalan Dhanaraman,^{†,‡} Ritta Mathew,[‡] and Dipankar Chatterji^{*,†}

[†]Molecular Biophysics Unit, Indian Institute of Science, Bangalore 560012, India

[‡]Institute of Life Sciences, University of Hyderabad campus, Gachibowli, Hyderabad 500046, India

S Supporting Information

ABSTRACT: Cyclic di-GMP (c-di-GMP), a ubiquitous bacterial second messenger, has emerged as a key controller of several biological processes. Numbers of reports that deal with the mechanistic aspects of this second messenger have appeared in the literature. However, the lack of a reporter tag attached to the c-di-GMP at times limits the understanding of further details. In this study, we have chemically coupled *N*-methylisatoic anhydride (MANT) with c-di-GMP, giving rise to Mant-(c-di-GMP) or MANT-CDG. We have characterized the chemical and physical properties and spectral behavior of MANT-CDG. The fluorescence of MANT-CDG is sensitive to changes in the microenvironment, which helped us study its interaction with three different c-di-GMP binding proteins (a diguanylate cyclase, a phosphodiesterase, and a PilZ domain-containing protein). In addition, we have shown here that MANT-CDG can inhibit diguanylate cyclase activity; however, it is hydrolyzed by c-di-GMP specific phosphodiesterase. Taken together, our data suggest that MANT-CDG behaves like native c-di-GMP, and this study raises the possibility that MANT-CDG will be a valuable research tool for the in vitro characterization of c-di-GMP signaling factors.



Cyclic di-GMP is a well-known bacterial second messenger, and enormous efforts have been spent to understand c-di-GMP signaling, which have been reported in many recent reviews.^{1,2} Comparatively, however, modifications of c-di-GMP were conducted infrequently^{3–5} to gain insight into the different stages of the biochemical pathways regulated by c-di-GMP. Some of these stages include production and interaction of c-di-GMP with various kinds of effectors and the control of intracellular c-di-GMP levels by cognate phosphodiesterases. Inhibition of these steps may provide an opportunity to control the deleterious outcome of c-di-GMP signaling.

For several decades, fluorescent analogues have been shown to be some of the most promising candidates for studying various steps (interactions and/or enzymatic activities) in biological processes. Some of these include AmNS-ppGpp, Mant-NTPs, Mant-cGMP, and Mant-cAMP.^{6–11} These fluorescent analogues have also been shown to be useful in studying the protein–ligand interaction and therefore result in determination of important kinetic parameters^{11,12} and in the development of potent inhibitors.¹³

In this study, we aimed to synthesize a fluorescent analogue of c-di-GMP, which can be useful in illuminating the mechanistic details of various pathways involving c-di-GMP. Mant (*N*-methylisatoic anhydride) was chosen because it is a very small fluorophore and is attached to the ribose moiety of the nucleotides in coupling reactions.⁷ Proteins that recognize Mant nucleotide analogues have been shown to be less sensitive

to alteration in the ribose moiety, when compared to that of base and phosphoryl moieties.^{7,11,14} These analogues showed very high quantum yields and resistance to photobleaching, and their absorption and emission spectra do not overlap with those of other biological molecules, especially proteins and nucleic acids.^{7,11}

Although di-MANT-(c-di-GMP) is commercially available from Biolog Co., in this study, we have conducted a simple and cost-effective synthesis of a singly labeled fluorescent analogue of c-di-GMP and named it MANT-(c-di-GMP) or MANT-CDG. We have studied various chemical and physical properties and spectral behavior of MANT-CDG. Steady state fluorescence spectroscopy was used to study the interaction between MANT-CDG and c-di-GMP signaling proteins (PleD, a diguanylate cyclase from *Caulobacter crescentus*; MSDGC-1, a bifunctional protein from *Mycobacterium smegmatis*; and YcgR, a PilZ domain-containing protein from *Escherichia coli*). Moreover, we report here that MANT-CDG inhibits the conversion of GTP to c-di-GMP by PleD; on the flip side, it is hydrolyzed by MSDGC-1. Using time-dependent fluorescence emission spectroscopy, a continuous real time monitoring of hydrolysis activity of MSDGC-1 was performed using MANT-CDG as a substrate and kinetic parameters for hydrolysis were approximated.

Received: March 19, 2012

Revised: June 19, 2012

Published: June 20, 2012



MATERIALS AND METHODS

Synthesis and Purification of Mant-(c-di-GMP). The coupling protocol was adapted from one published previously¹⁵ with slight modifications. Three milliliters of 0.5 mM c-di-GMP (procured from Nanyang Technological University, Singapore) in a 10 mL round-bottom flask was incubated in an oil bath at 38 °C, and the pH was adjusted to 9.6 with 1 N sodium hydroxide. The synthetic reaction was initiated by the addition of 105 mg of powdered *N*-methylisatoic anhydride (Mant) (Sigma). The pH was maintained at 9.6, every 10 min of the reaction. After 90 min, 105 mg of Mant was further added and incubated for an additional 90 min to increase the extent of product formation. Undissolved particles were removed by centrifugation at 5000 rpm for 10 min. The supernatant was transferred to a fresh tube and was extracted with an equal volume of chloroform. The aqueous phase was transferred to a fresh tube, and the pH was adjusted to 7.5 with 1 N acetic acid and filtered with a 0.22 μ m filter. This reaction mixture was stored at –80 °C until further use.

For purification of Mant-(c-di-GMP), 16 mL of diethylaminoethyl (DEAE)-cellulose from Sigma was packed in a Bio-Rad column connected to fast performance liquid chromatography (FPLC) system. The column was pre-equilibrated with buffer A [50 mM Tris-HCl (pH 7.5)] for 2 column volumes; 100 μ L of the reaction mixture was loaded onto the column, and unbound impurities were washed with 2 column volumes of buffer A with a flow rate of 1 mL/min. Elution was conducted with buffer B (1 M KCl in buffer A) following a linear gradient from 0 to 100% B over 10 column volumes. Eluted fractions were monitored at 254 nm, and peaks were collected and stored at –80 °C until further use. Desalting of the fractions was done manually with a Sephadex-G 10 column to remove the excess KCl.

To check the purity and for calculation of the retardation factor (R_f), purified fractions were run on a silica thin layer chromatography (TLC) sheet and developed in a 2-propanol/ammonia/water mixture (6:3:1, v/v/v, containing 0.5 g/L EDTA).⁷ Compounds were visualized by TLC with a UV illuminator at 254 and 365 nm.

Protein Expression and Purification. Proteins PleD, MSDGC-1, and YcgR were overexpressed and purified by growing *E. coli* BL21 [DE3 or pLys(s)] cells harboring the respective plasmids in LB broth with the antibiotic(s) (100 μ g/mL ampicillin or kanamycin or 34 μ g/mL chloramphenicol), induced with IPTG (isopropyl β -D-1-thiogalactopyranoside) (0.2 or 1 mM). Induced cells were harvested and lysed in lysis buffer [50 mM Tris (pH 7.9), 500 mM NaCl, 1 mM PMSF (phenylmethanesulfonyl fluoride), and 1 mg/mL lysozyme] followed by four to six rounds of sonication of 5 min each, with 2 s pulses at 4 °C. The lysate was cleared by centrifugation at 12000 rpm for 20 min at 4 °C, and the supernatant was loaded onto a Ni-NTA column pre-equilibrated with equilibration buffer [50 mM Tris-HCl (pH 7.9) and 500 mM NaCl]. The column was washed with 50 column volumes of wash buffer [50 mM Tris-HCl (pH 7.9), 500 mM NaCl, and 10 mM imidazole], and the protein was eluted out with elution buffer [50 mM Tris (pH 7.9), 500 mM NaCl, and 500 mM imidazole]. YcgR protein was further purified by using a Superdex-200 10/300 GL gel filtration column with buffer [50 mM Tris-HCl and 500 mM NaCl (pH 7.5)]. The eluted proteins were dialyzed against 25 mM Tris-HCl (pH 7.9), 250

mM NaCl, and 0.2 mM DTT and stored at 4 °C for further use, wherever required.

Effect of MANT-CDG on the Diguanylate Cyclase Activity of PleD. PleD (1 μ M) was preincubated with increasing concentrations of Mant-(c-di-GMP) (from 0 to 10 μ M) in a reaction buffer containing 25 mM Tris-HCl (pH 7.9), 250 mM NaCl, and 10 mM MgCl₂ in a 20 μ L reaction volume. Reactions were started by the addition of 100 μ M cold GTP and 1 μ L of [³²P]GTP [α -labeled [³²P]GTP (Board of Radiation and Isotope Technology (BRIT), India; 3500 Ci mmol^{–1}). Reactions were stopped after 30 min by boiling of the mixtures, and centrifugation was conducted at 12000 rpm for 10 min at room temperature. Supernatants were collected in fresh tubes, and 5 μ L of each was spotted on a polyethyleneimine-cellulose (PEI-cellulose) TLC plate (Merck). TLC was conducted in separation buffer [1:1.5 (v/v) saturated (NH₄)₂SO₄/1.5 M KH₂PO₄ (pH 3.6) mixture], and the plate was exposed to a phosphor-imager screen. Intensities of c-di-GMP spots were quantified using the MultiGauge tool. Data obtained in this study were fit in a dose–response model to yield the IC₅₀ value using GraphPad Prism 5.01.

Enzymatic Assay of MSDGC-1. To perform the phosphodiesterase assay using mass spectrometry, we started the reactions with purified protein MSDGC-1 in a reaction volume of 20 μ L containing 25 mM Tris-HCl (pH 7.9), 250 mM NaCl, and 5 mM MnCl₂, and the reactions were triggered by the addition of either c-di-GMP, MANT-CDG, or both, as per requirement. Reactions were stopped subsequently after fixed time intervals by boiling, and centrifugation was conducted at 12000 rpm for 10 min at room temperature. The supernatant was collected in fresh tubes, concentrated by vacuum evaporation, and analyzed by mass spectrometry.

Mass Spectrometry. For mass spectrometric studies, an Ultraflex TOF-TOF mass spectrometer (Bruker Daltonics) was used; calibration was done using the standard calibration kit provided by the manufacturer. Samples were mixed with a solution containing 10 mg of α -cyano-4-hydroxycinnamic acid (CCA) per milliliter and 50% (v/v) acetonitrile (ACN). One microliter of every sample was spotted onto a MALDI-TOF MS (matrix-assisted laser desorption/ionization time-of-flight mass spectroscopy) plate and analyzed in negative or positive ion mode, whenever necessary.

Absorption and Fluorescence Spectroscopy. Absorption spectra were recorded in Varian Cary 100 Bio UV–visible spectrophotometer. Samples were placed in 25 mM Tris-HCl (pH 7.5) and 250 mM KCl or NaCl and scanned from 240 to 400 nm in a 1 cm cell. Steady state fluorescence spectra were recorded with a Fluorolog-Tau III spectrofluorimeter (having a Xe lamp as the excitation source and spectral correction facility) (Jobin Yvon) or a Jasco FP-6300 spectrofluorimeter using an excitation wavelength of 295 or 355 nm in a 10 mm path length cell. All measurements for fluorescence were taken in a buffer [25 mM Tris-HCl (pH 7.5) and 250 mM KCl or NaCl] with or without 5 mM MgCl₂ or MnCl₂. The buffer background was subtracted wherever required in both absorption and fluorescence experiments. All the experiments were repeated in a minimum of three independent batches. Binding of MANT-CDG with PleD, MSDGC-1, and YcgR was monitored using a protocol, which was adapted from the work of others¹² with slight modifications. An excitation wavelength of 295 and 355 nm was used in the case of FRET or the measurement of direct fluorescence, respectively. For the steady state

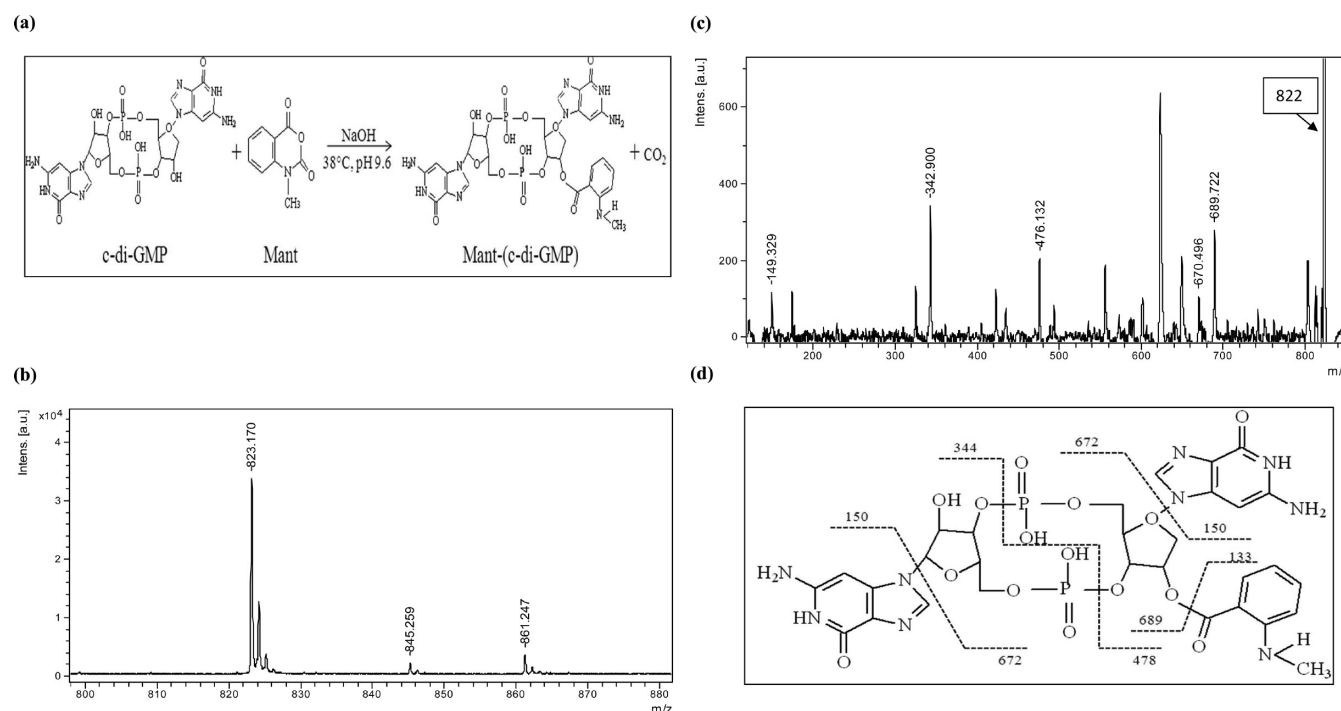


Figure 1. Synthesis and structural validation of Mant-(c-di-GMP) or MANT-CDG. (a) Schematic representation of coupling of Mant with c-di-GMP. (b) MALDI-TOF spectrum of purified MANT-CDG in negative ion mode showing peaks at m/z 823 ($M - H$)⁻, m/z 845 ($M - H + Na$)⁻, and m/z 861 ($M - H + K$)⁻. (c) MALDI-TOF (MS/MS) spectrum showing fragmentation of MANT-CDG where peaks at m/z 149, 670, and 689 correspond to products after single-bond cleavage and peaks at m/z 342 and 476 correspond to products after double-bond cleavage (spectra recorded in negative ion mode). (d) Ion fragmentation pattern after single- and double-bond cleavage in MS/MS as described for panel c. Dotted lines represent cleavage sites.

fluorescence anisotropy measurement, equimolar concentrations (500 nM) of MANT-CDG and YcgR were mixed and incubated, and values were acquired using excitation and emission wavelengths of 355 and 440 nm, respectively. The dissociation constant for binding of MANT-CDG with YcgR was determined by measuring emission at 440 nm when samples were excited at 295 nm (FRET) as suggested previously.¹² The samples were prepared by the addition of increasing concentrations of MANT-CDG (0.1–2.0 μ M) with a fixed amount of protein (1 μ M). Data obtained were best fit in single-binding site and specific interaction mode using GraphPad Prism 5.01. For competition experiments, an excess of native c-di-GMP (~40–100-fold) was added to the reaction mixture containing protein and MANT-CDG.

Calculation of the Distance between the Tryptophan Residue of MSDGC-1 and MANT-CDG. The FRET distance between the donor (Trp) and the acceptor (MANT-CDG) was calculated from the change in the quantum yield of the donor in the presence of the acceptor following the well-known Förster equation¹⁶ and our previous work.¹⁷

The transfer efficiency (E) was calculated by using the formula

$$E = 1 - Q_{DA}/Q_D \quad (1)$$

where Q_{DA} and Q_D are the quantum yields of the donor in the presence and absence of the acceptor, respectively.

The characteristic transfer distance (R_0), at which the transfer efficiency equals 50%, was calculated by using the formula

$$R_0 = 9.79 \times 10^3 \times [JQ(n^{-4}\kappa^2)]^{1/6} \quad (2)$$

where n is the refractive index of the medium (1.4) and κ^2 represents the orientation factor, which was taken to be $2/3$ considering the isotropic nature of the donor. The sixth-root dependence of R_0 on κ^2 limits the error within 20%.

Finally, the distance (r) between the donor tryptophan and MANT-CDG was determined by using the formula

$$r = R_0(1/E - 1)^{1/6} \quad (3)$$

Real-Time Monitoring of the Hydrolysis Activity of MSDGC-1. The protocol was essentially described previously¹⁸ with slight modifications. In brief, the reaction was conducted with 4 μ M MSDGC-1 in a reaction buffer containing 25 mM Tris-HCl (pH 7.5), 250 mM NaCl, 0.2 mM DTT, and 5 mM MnCl₂ in a Jasco FP-6300 spectrofluorimeter. The reaction was started by the addition of 0.4 μ M MANT-CDG, and the decrease in fluorescence at 440 nm was measured for 40 min in time-dependent experiments. Data points obtained in these studies were fit to a single-exponential decay curve using GraphPad Prism 5.01 for the analysis of the kinetic parameters.

Bioinformatics Analysis, Structural Modeling, and Model Validation. The sequence and structure of PleD from *Caulobacter* were obtained from the NCBI and PDB, respectively. PleD (PDB entry 1W25) with bound c-di-GMP¹⁹ was used in this case to show the allosteric inhibition site and the electrostatic surface. The sequence of MSDGC-1 (615 amino acids) was obtained from KEGG (Kyoto Encyclopedia of Genes and Genomes) (http://www.genome.jp/dbget-bin/www_bget?msm:MSMEG_2196), and boundaries of the EAL domain (residues 353–590) were determined using PFAM (<http://pfam.sanger.ac.uk/search/sequence>). The structural model of the EAL domain was built using SWISS MODEL²⁰

with PDB entry 2R6O as the template (the coordinates of the tREAL structure, chain A, 39.331% identical). PROCHECK²¹ was used to validate the modeled structure in which more than 90% of the residues fall into the favorable region of the Ramachandran plot. Visualization of the three-dimensional structure was achieved using PyMOL.

RESULTS

Synthesis, Purification, and Validation of Mant-(c-di-GMP) or MANT-CDG. In this study, we have synthesized c-di-GMP tagged with the Mant group. In this case, the Mant group was expected to be covalently linked with the 2'-oxygen of the ribosyl moieties in c-di-GMP with the loss of CO₂ (Figure 1a), as reported previously.^{7,11} End products of the reaction were analyzed by mass spectrometry, which shows the presence of unreacted c-di-GMP and singly and doubly labeled c-di-GMP (Figure S1a of the Supporting Information). The presence of the prominent peak at (mass/charge) m/z 824 $[M + H]^+$ indicates the high yielding nature of the reaction for singly labeled c-di-GMP. To purify monolabeled c-di-GMP, we loaded the reaction mixture onto the FPLC column. One of the eluted peaks showed the presence of monolabeled c-di-GMP or Mant-(c-di-GMP), which was then desalted, identified by mass spectrometry with a value of m/z 823 $[M - H]^-$ (Figure 1b).

To confirm that labeling of the Mant group has taken place at the 2'-oxygen of the ribosyl moiety, singly labeled c-di-GMP was treated with acid and products were analyzed through mass spectrometry. We noticed the presence of the protonated mass of c-di-GMP indicating the complete hydrolysis of the ester bond between c-di-GMP and the Mant group at the 2'-oxygen of the ribosyl moiety in the c-di-GMP (Figure S1b of the Supporting Information). To further analyze the structure of Mant-(c-di-GMP), MALDI-TOF (MS/MS) analysis was performed. Panels c and d of Figure 1 show the presence of fragmentation products and the ion fragmentation pattern, respectively. We were able to identify most of the major ions upon fragmentation, which confirmed both labeling and structure. Similar studies have been performed by others to confirm the structure of c-di-GMP²² and c-di-AMP.^{23,24} Singly labeled c-di-GMP or Mant-(c-di-GMP) was used for all the experiments reported in this study and named MANT-CDG for the sake of convenience.

Physicochemical and Spectral Characterization of MANT-CDG. Fluorescent analogues are often the molecule of choice in various biochemical studies; however, the demand for its use lies exclusively in various extraordinary properties shown by these probes. While characterizing MANT-CDG, we first noticed that the R_f value (retardation factor) of MANT-CDG is 0.74, significantly different from that of unlabeled c-di-GMP (0.60). MANT-CDG was found to be stable between pH 4 and 9.6 and resistant to heat (95 °C, both for 30 min) (Figure S2 of the Supporting Information). The absorption spectrum of MANT-CDG exhibits two maxima at 254 and 355 nm and a shoulder at ~280 nm (Figure 2a). The broad band at 355 nm is associated with the Mant group as pure c-di-GMP does not show this peak.

MANT-CDG [in buffer containing 25 mM Tris-HCl (pH 7.5), 250 mM NaCl, and 0.2 mM DTT] was excited at 355 nm and showed strong fluorescence with an emission maximum at ~440 nm (Figure 2b). It showed a large Stokes shift of ~90 nm (data not shown), and fluorophores with large Stokes shifts are widely used as they are less likely to self-quench by homotransfer of fluorescence between the same two

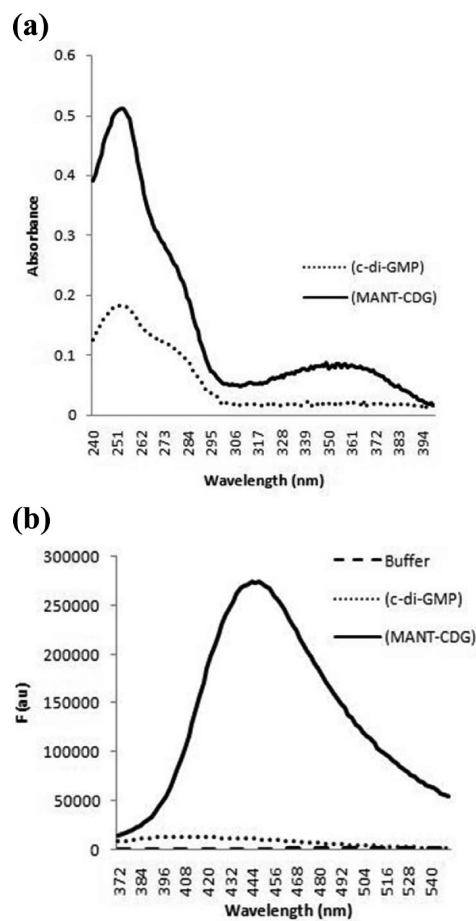


Figure 2. Spectroscopic characterization of MANT-CDG. (a) UV-visible absorption spectrum of MANT-CDG. (b) Fluorescence spectrum of MANT-CDG. MANT-CDG emits around 440 nm upon excitation at 355 nm.

fluorophores. Additionally, MANT-CDG was found to be highly soluble in water in contrast to Mant. We also noticed that the presence or absence of divalent cations like Mg²⁺ or Mn²⁺ had no significant effect on the fluorescence emission of MANT-CDG (data not shown).

Further, we conducted physicochemical characterization in greater detail. We observed that when the polarity was changed because the solvent was changed from water to ethanol or DMF (dimethylformamide) (from 0 to 80%), the fluorescence intensity increases with a blue shift of ~10 or ~18 nm, respectively (Figure S3a,b of the Supporting Information). This indicates that the fluorescence of MANT-CDG is sensitive to a change in the microenvironment. Interestingly, its fluorescence is optimal at physiological pH (~7), and emission maxima do not change with pH, indicating that only one emissive species of MANT-CDG is responsible for the fluorescence (Figure S3c,d of the Supporting Information). Upon exposure of MANT-CDG to normal daylight, an only 8% decrease in emission maxima was noticed after 10 h (Figure S4a of the Supporting Information). The intermittent exposure of MANT-CDG to light at its excitation wavelength (every 6 min) resulted in a decrease in fluorescence of only 10% in 1 h (Figure S4b of the Supporting Information), suggesting that MANT-CDG is an extremely photostable molecule.

Studies of the Interaction of MANT-CDG with c-di-GMP Binding Proteins. In the c-di-GMP-dependent down-

stream signaling pathways, the effect of cellular concentrations of c-di-GMP is relayed upon its binding with a variety of effectors (receptors or target molecules). These effectors can be classified into two categories on the basis on their inherent activities:^{1,2} (a) various protein receptors,¹ including those having a PilZ domain or a degenerate GGDEF or EAL domain, and (b) RNA molecules with c-di-GMP binding signature motifs (GEMM). Monomeric or dimeric forms of c-di-GMP bind to these effectors and confer upon them altered activity. We observed here that the fluorescence of MANT-CDG is sensitive to its ambience, and there is a significant change in the emission with changes in the microenvironment. Thus, we planned to see if MANT-CDG can be used to study the interaction between c-di-GMP and its effectors by means of fluorescence spectroscopy. For this purpose, we overexpressed and purified (Figure S5 of the Supporting Information) three structurally, functionally, or catalytically unrelated proteins and performed the binding experiments that are described below.

Interaction with PleD and Inhibition of Diguanylate Cyclase Activity. PleD (a bona fide diguanylate cyclase) has an allosteric inhibition site called a primary inhibition site (Ip site with the RxxD motif found five amino acids upstream of the A site with the GGDEF motif) and a secondary inhibition site (Is site), where c-di-GMP binds with very high affinity and immobilizes the protein in an inactive state. This mechanism of allosteric control (making a protein inactive by “domain immobilization”) was suggested for the regulation of intracellular levels of c-di-GMP.^{19,25,26} This product inhibition site was exploited here to study the interaction of MANT-CDG and PleD, which was confirmed by the change in fluorescence emission of MANT-CDG when reaction mixtures containing both were excited at 355 nm. We were able to observe a large increase in the fluorescence emission of MANT-CDG upon incubation with PleD, which was abrogated in the presence of excess native c-di-GMP (Figure 3a). This experiment suggested specific interaction between MANT-CDG and PleD like that of unlabeled c-di-GMP and PleD. A further experiment as described below confirmed that the modes of interaction of PleD with native c-di-GMP and PleD with MANT-CDG are similar in nature. A diguanylate cyclase (DGC) assay of PleD was performed via radiometric experiments using GTP as a substrate in the presence of MANT-CDG. We observed a decrease in the synthesis activity of PleD as a function of an increasing MANT-CDG concentration, and the IC₅₀ was calculated to be $5.18 \pm 0.2 \mu\text{M}$ (Figure 3b). Therefore, MANT-CDG binds with PleD having an affinity and a mode of inhibition similar to those of native c-di-GMP.²⁶ Similar modes of inhibition by nonfluorescent analogues of c-di-GMP have been reported recently.^{5,27}

Binding with MSDGC-1 and Determination of the Distance between the Donor (Trp) and Acceptor (MANT-CDG) by Förster's Energy Transfer. MSDGC-1 is a bifunctional enzyme from *M. smegmatis*, which has both DGC and PDE activity.²⁸ Because MSDGC-1 does not have a product inhibition site (data not shown), MANT-CDG is supposed to bind only with the EAL domain. To follow the interaction between the EAL domain of MSDGC-1 and MANT-CDG, first a fluorescence resonance energy transfer (FRET)-based method was adapted. The emission spectrum of MSDGC-1 has significant spectral overlap ($J = 6.03 \times 10^{-14} \text{ M}^{-1} \text{ cm}$) with the absorption spectrum of the Mant group in MANT-CDG (Figure S6a of the Supporting Information and Table 1), and thus, they can be used as an excellent donor–acceptor pair. It

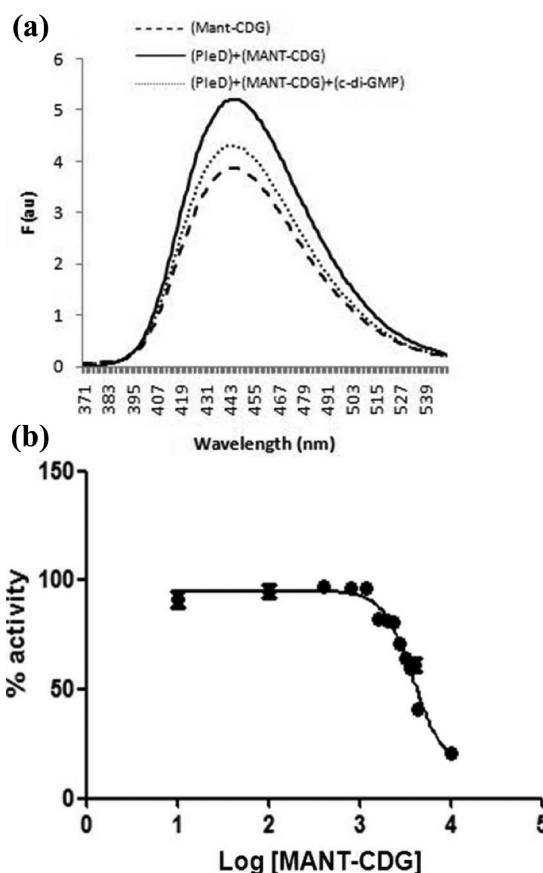


Figure 3. MANT-CDG can bind to PleD and inhibit the diguanylate cyclase activity. (a) Increase in fluorescence upon interaction of MANT-CDG with PleD, which is reversed by the addition of native c-di-GMP. Samples were excited at 355 nm, and spectra were recorded in the presence of 10 mM MgCl₂. All the spectra were blank subtracted. (b) Inhibitory effect of MANT-CDG on the diguanylate cyclase activity of PleD (see Materials and Methods).

can be seen from Figure 4a that there are five tryptophan residues in MSDGC-1, of which three fall in the EAL domain. In addition, the amino acid sequence analysis (Figure 4b) of the EAL domain of MSDGC-1 showed that three important amino acids (R338, D507, and D529) are conserved in this region for binding to c-di-GMP as shown previously.²⁹ Via structural modeling of the EAL domain of MSDGC-1, we observed that all three tryptophans are placed near the c-di-GMP binding site (Figure 4c).

Indeed, upon excitation of the samples containing MSDGC-1 and MANT-CDG at 295 nm, the typical tryptophan fluorescence was observed followed by the emission of the Mant group at ~440 nm indicating Förster's energy transfer (Figure 4d). It also shows one isoemissive point at 410 nm, indicating the formation of a 1:1 complex between MSDGC-1 and MANT-CDG. It should be mentioned here that MANT-CDG binds with the EAL domain of MSDGC-1 and is catalytically converted to labeled pGpG by the hydrolysis activity over a longer time course. We will demonstrate that this activity requires the presence of a divalent cation. We noticed that the binding of MANT-CDG to MSDGC-1 and subsequent energy transfer can take place without a divalent cation. However, in the presence of a divalent cation, the binding experiment can be performed within 2 min without appreciable hydrolysis.

Table 1. Calculation of the Distance between a Donor–Acceptor Pair by Förster Resonance Energy Transfer

sample	excitation wavelength (nm)	emission wavelength (nm)	spectral overlap integral J ($M^{-1} cm^3$)	quantum yield Q	distance at 50% energy transfer efficiency R_0 (Å)	energy transfer efficiency E	distance between the donor and acceptor, r (Å)
MSDGC-1	295	340		0.015			
MSDGC-1 with MANT-CDG	295	340	6.03×10^{-14}	0.013	23.3	0.14	32.2

(a)



(b)

Sequence alignment of the EAL domain of MSDGC-1 with well-studied EAL domain proteins RocR and tdEAL from *Pseudomonas aeruginosa* and *Thiobacillus denitrificans*, respectively. Conserved c-di-GMP binding residues are indicated by arrows, and tryptophan residues of the EAL domain of MSDGC-1 are highlighted in gray.

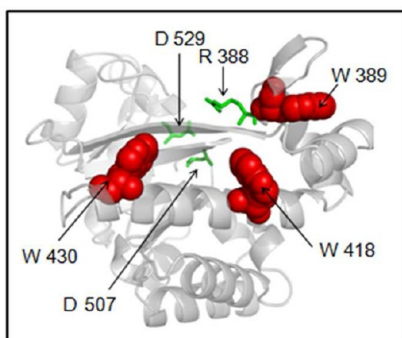
```

MSDGC-1      EGGALVLHYLPIDMRTGEVLAAEALVRWEHPTRGLLSPDSFIGVAESINLAGELGRWVL 420
tdEAL        ERNELVLHYQPIVELASGRIVGGEALVRWEDPERGLVMPSAFIPAAEDTGLIVALSDWVL 95
RocR         DNGEFEAYYQPKVALDGGGLIGAEVLARWNHPLGLVLPSPSHFLYVMETYNLVDKLFWQLF 211
               : . : : * * : : * : . . . * . * . : . * * : . * * : . * * : . :

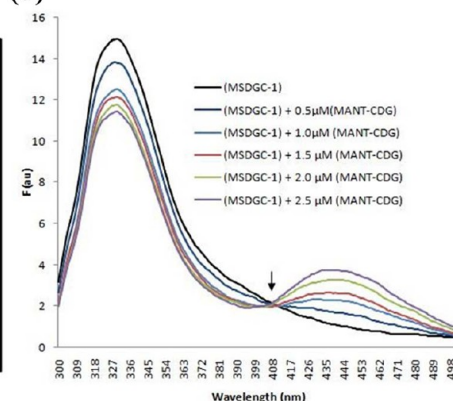
MSDGC-1      RTACAEFSRWWRANG-VGRNIVLRINVSFVQLVTDGFVESVAGIMKEFGLPRGSVCLEITE 479
tdEAL        EACCTQLRAWQQQGRAADDLTLSVNISTRQFEGEHLTRAVDRALARSGLRPDCLELEITE 155
RocR         SQGLATRRKLAQLG---QPINLAFNVHPSQLGSRALAENISALLTEFHLPPSSVMFEITE 268
               :      *      : * . * : * :      : . :      : . *      : . : * * *

MSDGC-1      SVVVQDIETTRTTLTGLHNVGVQVAIDDFGTGYSVLSLLKSLPVDTLKIDRSFVAELGSN 539
tdEAL        NVMLVMTDEVRTCLDALRARGVRLALDDFGTGYSSLSYLSQLPFHGLKIDQSFRVKIPAH 215
RocR         TGLISAPASSLENLVRIRMGCGLAMDDFGAGYSSLDRLCEFFPSQIKLDRTFVQRMKTQ 328
               . : :      * * : * : * : * * : * * : * . * . : . : * : * : * : * : :
    
```

(c)



(d)



(e)

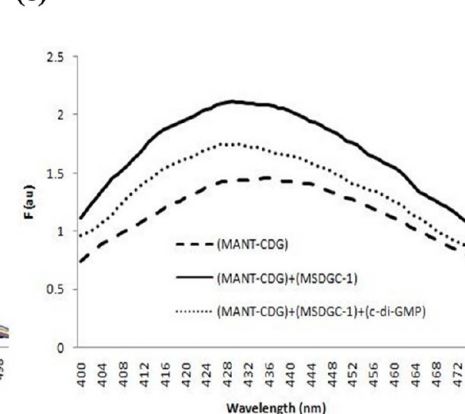


Figure 4. Interaction of MANT-CDG with MSDGC-1. (a) Domain architecture of MSDGC-1 showing the distribution of tryptophan residues at various positions (three tryptophan residues are present in the EAL domain). (b) Sequence alignment of the EAL domain of MSDGC-1 with well-studied EAL domain proteins RocR and tdEAL from *Pseudomonas aeruginosa* and *Thiobacillus denitrificans*, respectively. Conserved c-di-GMP binding residues are indicated by arrows, and tryptophan residues of the EAL domain of MSDGC-1 are highlighted in gray. (c) Modeled structure of the EAL domain of MSDGC-1 showing the close appearance of tryptophan residues near the c-di-GMP binding site. (d) Fluorescence emission showing FRET between MSDGC-1 and MANT-CDG upon excitation at 295 nm in the absence of a divalent cation. It also shows an isoemissive point at ~410 nm (indicated by an arrow). (e) Decrease in fluorescence of MANT-CDG bound with MSDGC-1 as c-di-GMP competes with MANT-CDG for the binding site on MSDGC-1. Spectra were recorded in the absence of a divalent cation.

In another approach, the direct fluorescence of MANT-CDG when bound with MSDGC-1 was also measured by exciting samples at 355 nm, and there was a large increase in the emission of MANT-CDG at ~440 nm (Figure 4e). Hence, both FRET and direct fluorescence measurement experiments confirmed interaction of MANT-CDG with MSDGC-1. Importantly, we also noticed that native c-di-GMP in excess

can compete with MANT-CDG from the MSDGC-1–MANT-CDG complex in both cases of direct fluorescence measurement (Figure 4e) and FRET experiment (Figure S6b of the Supporting Information). This was obvious because of the decrease in the fluorescence of the reaction mixture containing MANT-CDG and MSDGC-1 in the presence of excess native

c-di-GMP, which also suggests a specificity of interaction of MANT-CDG with MSDGC-1.

To gain insight into the interaction between the EAL domain of MSDGC-1 and MANT-CDG, we used data obtained in FRET experiments to estimate the distance between the donor tryptophan residue, which forms a Förster pair, and the acceptor MANT-CDG through nonradiative energy transfer. Values of the quantum yield of the samples were determined and are summarized in Table S1 of the Supporting Information. The acceptor probe (MANT-CDG) was found to be 32.2 Å from the donor tryptophan (W418) (Table 1). The modeled structure of the EAL domain was used to cross check this value and found to be close to that obtained experimentally (Table S2 of the Supporting Information).

Studies of Interaction with a PilZ Domain-Containing Protein, YcgR. The PilZ domain was first hypothesized to bind with c-di-GMP by Amikam and Galperin using bioinformatics analysis,³⁰ which was subsequently established as a bona fide adaptor for c-di-GMP by others.^{31–33} In this study, we have studied interaction of MANT-CDG with a PilZ domain-containing protein, YcgR from *E. coli*. YcgR is a two-domain protein in which c-di-GMP binds at the N-terminus of the C-terminal PilZ domain. This binding results in a large conformational change, which activates the protein.^{31,33} Because YcgR has three tryptophan residues (including one in the PilZ domain), the binding studies were performed with pure protein and MANT-CDG as shown in the case of MSDGC-1. In the direct fluorescence experiment, excess native c-di-GMP was found to compete with MANT-CDG from YcgR, suggesting a specificity of interaction (Figure 5a). Further, fluorescence anisotropy measurements were taken to substantiate the aforementioned binding (Figure 5b). The anisotropy of MANT-CDG increases when it binds with the protein, which is lowered in the presence of excess native c-di-GMP. Moreover, a FRET experiment was performed with increasing concentrations of MANT-CDG, keeping constant the amount of protein as reported previously.¹² Data obtained at 440 nm in these studies were fit in one binding site and specific interaction mode using GraphPad Prism 5.01, and the dissociation constant for the interaction of MANT-CDG with YcgR was found to be 572.4 nM (Figure 5c).

Assessment of the Microenvironment of the c-di-GMP Binding Site on PleD and MSDGC-1. To assess the nature of the binding site of c-di-GMP on PleD and MSDGC-1, fluorescence quenching experiments were performed using acrylamide and potassium iodide (KI), as reported previously.^{11,34} Acrylamide, being a neutral quencher molecule, can sense the hydrophobic environment, and iodine, being negatively charged, can sense the polar or charged environment of the fluorophore binding site. We observed that the fluorescence emission of MANT-CDG bound to PleD is quenched to a lesser extent than that of free MANT-CDG by KI, suggesting that MANT-CDG was partially solvent accessible. However, quenching by acrylamide was stronger than that by KI for MANT-CDG bound with PleD (Figure 6a,b), indicating the presence of hydrophobic character in the binding site of MANT-CDG on PleD. The structure of c-di-GMP-bound PleD supports the findings that the c-di-GMP binding site (I-site) on PleD is partially solvent exposed (Figure S7a of the Supporting Information). To further substantiate our observation, the electrostatic surface for the c-di-GMP binding site on PleD was generated, and it is evident that the surface is charged or polar and surrounded by hydrophobic residues

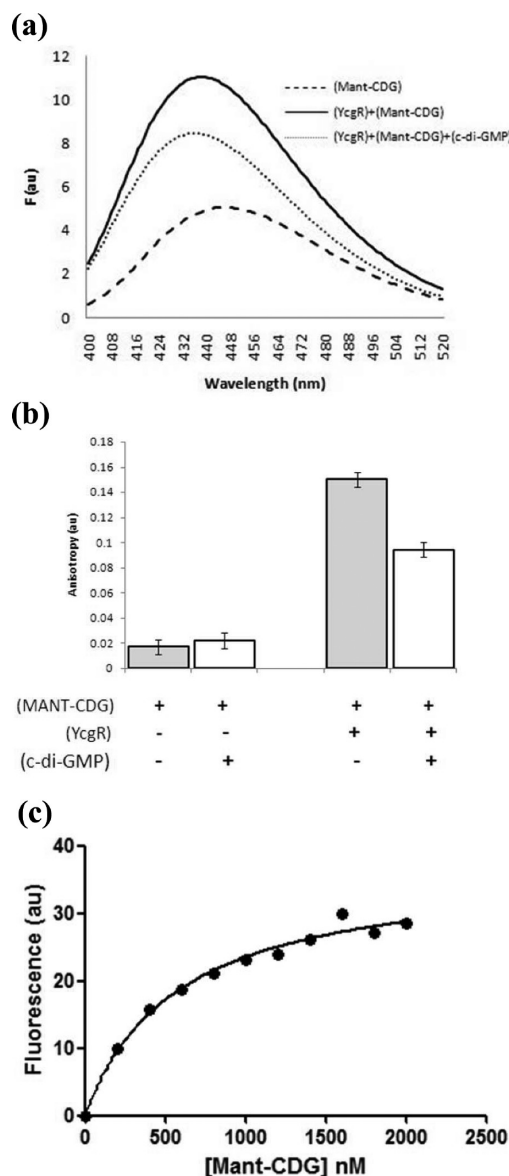


Figure 5. Binding of MANT-CDG with YcgR. (a) Direct fluorescence measurement upon interaction of MANT-CDG with YcgR upon excitation at 355 nm. This fluorescence is diminished by the presence of excess native c-di-GMP, suggesting a specificity of this interaction. (b) Increment in the fluorescence anisotropy value of MANT-CDG upon binding with YcgR. (c) Saturation binding of MANT-CDG with YcgR.

(Figure S7b of the Supporting Information). A similar study was conducted to investigate the binding site of c-di-GMP on the EAL domain of MSDGC-1. Fluorescence quenching by acrylamide was found to be stronger than that by KI, suggesting that the c-di-GMP binding site on the EAL domain of MSDGC-1, despite having some hydrophobic character, is more solvent accessible than that of PleD (Figure 6c,d). This experiment indicates that the catalytic function of a phosphodiesterase requires easy accessibility of the substrate.

Approximation of the Kinetic Parameter for the Phosphodiesterase Activity of MSDGC-1. It has been observed that Mant-GTP was acting as an inhibitor of the diguanylate activity of YdeH from *E. coli* (an enzyme that catalyzes the synthesis of c-di-GMP using substrate GTP).¹³ Similarly, we were interested in finding out if Mant-CDG can

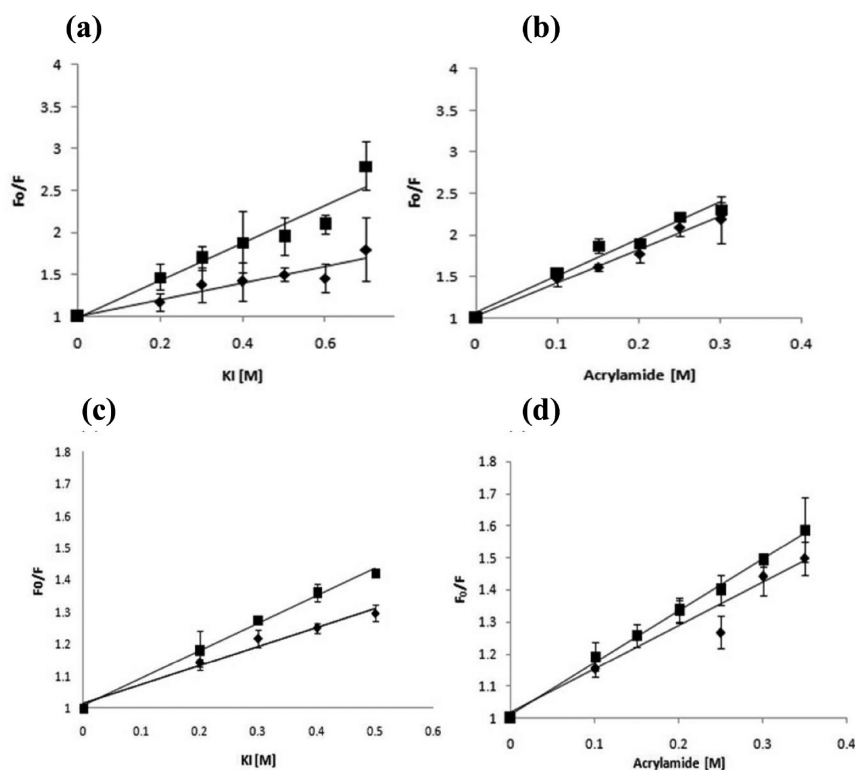


Figure 6. Stern–Volmer plot showing the microenvironment of the c-di-GMP binding site on PleD and MSDGC-1 as indicated by fluorescence quenching. Squares and diamonds represent quenching of free MANT-CDG and MANT-CDG bound with PleD (a and b) or MSDGC-1 (c and d), in the presence of KI or acrylamide, respectively.

act as an inhibitor of the phosphodiesterase activity of MSDGC-1. To investigate this, we monitored the phosphodiesterase activity with native substrate c-di-GMP in the presence of MANT-CDG. Surprisingly, both c-di-GMP and MANT-CDG were found to be hydrolyzed as confirmed by the appearance of two new peaks in the mass spectrometric analysis at m/z 709 ($M + H$)⁺ (pGpG, hydrolysis product of c-di-GMP) and m/z 842 ($M + H$)⁺ (MANT-pGpG, hydrolysis product of MANT-CDG) when compared with control (Figure 7a, i and ii). The phosphodiesterase activity with MANT-CDG alone was also determined, which was found to be hydrolyzed as well (Figure 7a, iii and iv). A divalent cation ($MnCl_2$) was found to be essential for activity; without it, no hydrolysis was observed (Figure 7a, v).

Our experiments showed that MANT-CDG is not an inhibitor but acts as a substrate for phosphodiesterase with an active EAL domain. This prompted us to develop a method for continuous real-time monitoring of the phosphodiesterase activity of MSDGC-1. The method was essentially taken from the work of Sullivan et al.,¹⁸ in which they reported hydrolysis of Mant-GTP to Mant-GDP by a protein Era using time course fluorescence spectroscopy. As with their observation, we found higher fluorescence emission for the bound substrate (MANT-CDG) than for the bound product (MANT-pGpG) with MSDGC-1 (Figure 7b). We took advantage of this significant difference for determining the values of kinetic parameters for hydrolysis of MANT-CDG by MSDGC-1 in the presence of $MnCl_2$. We developed an assay with a 10-fold lower MANT-CDG concentration compared to that of the protein, so that binding of most of the substrate takes place at the beginning of the measurement. Thus, the conversion of the substrate to the product will result in a decrease in fluorescence that can be

monitored as a function of time. Indeed, we were able to monitor the decrease in fluorescence over time (Figure 7c). The product was also identified by mass spectrometry to confirm the progress of hydrolysis under similar conditions (data not shown). Data points obtained in fluorescence experiments were fit to a single-exponential decay curve using GraphPad Prism 5.01, and approximate kinetic parameters were determined. Values of V_{max} and K_m were calculated to be 2.5 nM min^{−1} and 270 nM, respectively, and found to be in the range of previously reported parameters for different c-di-GMP specific phosphodiesterases.^{29,35,36} Therefore, MANT-CDG can be used to monitor the hydrolysis activity of c-di-GMP specific phosphodiesterases in real-time experiments without much change in affinity.

DISCUSSION

We have successfully synthesized, purified, and characterized the fluorescent analogue of c-di-GMP called Mant-(c-di-GMP) or MANT-CDG. The position of the fluorophore is well-defined here, which makes it a conformationally suitable probe for biophysical studies. Various chemical and physical properties and the spectral behavior of MANT-CDG showed that it can act as good probe for addressing biological questions involving c-di-GMP. An interesting and important feature that emerged here is that the modification of c-di-GMP at one of the ribosyl moieties does not affect its binding with three structurally and catalytically or functionally different proteins. This was obvious because MANT-CDG can interact with these proteins in a fashion similar to that of native c-di-GMP. Therefore, we propose that MANT-CDG can be used to study interaction with a variety of other c-di-GMP binding partners, as well (for example, proteins with degenerate GGDEF or EAL

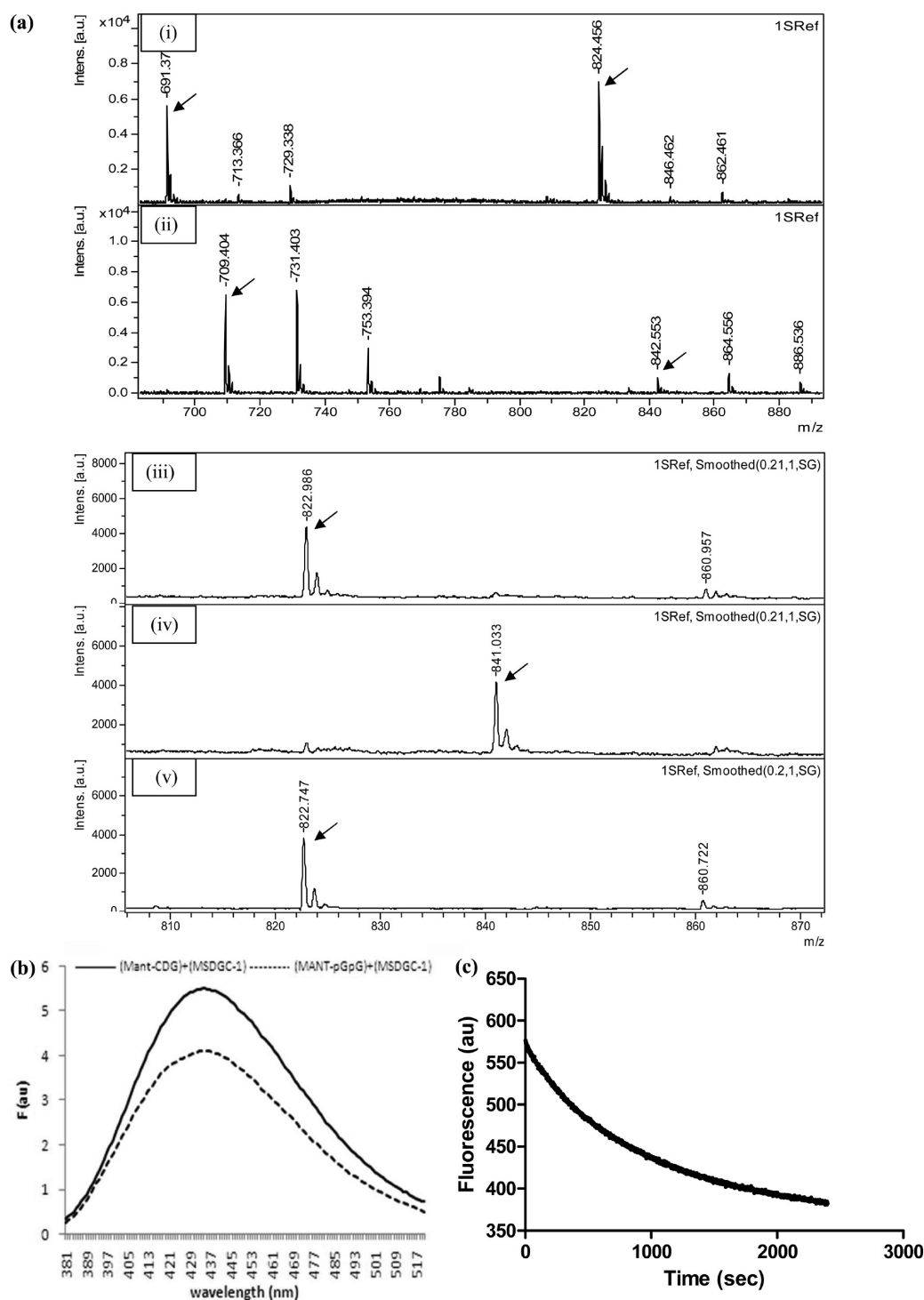


Figure 7. Real-time monitoring of the phosphodiesterase activity of MSDGC-1 using MANT-CDG as a substrate. (a) Mass spectrometric analysis showing the phosphodiesterase activity of MSDGC-1 for MANT-CDG. (i) Control reaction mixture showing the presence of *c*-di-GMP [m/z 691($M + H$)⁺] and MANT-CDG [m/z 824 ($M + H$)⁺] in the absence of MSDGC-1. (ii) Hydrolysis products pGpG [m/z 709 ($M + H$)⁺] and Mant-pGpG [m/z 842 ($M + H$)⁺] in the presence of MSDGC-1 and $MnCl_2$. (iii) Control MANT-CDG [m/z 822.98 ($M - H$)⁻]. (iv) Hydrolysis product of MANT-CDG, Mant-pGpG [m/z 841.03 ($M - H$)⁻] in the presence of $MnCl_2$ (5 mM) and MSDGC-1. (v) No hydrolysis product can be seen in the absence of $MnCl_2$, showing importance of the metal in catalysis. (b) Fluorescence spectra showing the difference in the fluorescence emission of bound MANT-CDG and bound MANT-pGpG with MSDGC-1. (c) Time-dependent change in the fluorescence emission at 440 nm, when excited at 355 nm, to monitor hydrolysis activity of MSDGC-1 using MANT-CDG as a substrate (see Materials and Methods).

domain and RNA molecules), without much change in affinity. *c*-di-GMP affects the biofilm, virulence, and related diseases, and hence, developing and screening an inhibitor for *c*-di-GMP-mediated signaling pathways is important. MANT-CDG

provides insights into such possibilities as it can act as a fluorescent substrate for studying the kinetics of *c*-di-GMP specific phosphodiesterases. This assay can be performed in real time, which provides insight into the catalytic mechanism. To

the best of our knowledge, MANT-CDG is the first fluorescent analogue of c-di-GMP, which shows significant potential for the study of c-di-GMP signaling.

■ ASSOCIATED CONTENT

● Supporting Information

Tables S1 and S2 and Figures S1–S7. This material is available free of charge via the Internet at <http://pubs.acs.org>.

■ AUTHOR INFORMATION

Corresponding Author

*Molecular Biophysics Unit, Indian Institute of Science, Bangalore 560012, India. E-mail: dipankar@mbu.iisc.ernet.in. Telephone: +91-80-22932836. Fax: +91-80-23600535.

Author Contributions

I.M.S. and T.D. have contributed equally to this work.

Funding

This work was funded by a Centre for Excellence grant from the Department of Biotechnology (DBT), Government of India, to D.C. I.M.S. thanks the Council of Scientific and Industrial Research (CSIR), Government of India, for providing a Senior Research Fellowship (SRF). T.D. thanks Department of Biotechnology (DBT), Government of India, for a Junior Research Fellowship (JRF).

Notes

The authors declare no competing financial interest.

■ ACKNOWLEDGMENTS

R.M. thanks ILS, Hyderabad, and DBT for the facilities and support. Our sincere thanks to Prof. Urs Jenal (Biozentrum, Zurich, Switzerland) and Prof. Mark Gomelsky (University of Wyoming, Laramie, WY) for kindly providing clones of PleD and YcgR, respectively. Binod Kumar Bharati, Thyageshwar C., Prasun Kumar, Kuldeepkumar Gupta, Dr. Sanjay Kasetty, and Anjaney Kothari are acknowledged for suggestions, help in running protein gels, and bioinformatics analysis. Sathisha K. and Sunitha P. are acknowledged for their consistent help with mass spectrometry.

■ ABBREVIATIONS

c-di-GMP, cyclic di-guanosine monophosphate; c-di-AMP, cyclic di-adenosine monophosphate; Mant, *N*-methylisatoic anhydride; DGC, diguanylate cyclase; MANT-CDG, Mant-cyclic di-guanosine monophosphate; AmNS, aminonaphthalenesulfonic acid; ppGpp, guanosine tetraphosphate; NTP, nucleotide triphosphate; cAMP, cyclic adenosine monophosphate; cGMP, cyclic guanosine monophosphate; GTP, guanosine triphosphate; DEAE-cellulose, diethylaminoethyl-cellulose; FPLC, fast performance liquid chromatography; KCl, potassium chloride; TLC, thin layer chromatography; EDTA, ethylenediaminetetraacetic acid; UV, ultraviolet; IPTG, isopropyl β -D-1-thiogalactopyranoside; PMSF, phenylmethanesulfonyl fluoride; Ni-NTA, nickel-nitrilotriacetic acid; DTT, dithiothreitol; BRIT, Board of Radiation and Isotope Technology; PEI-cellulose, polyethyleneimine-cellulose; MALDI-TOF MS, matrix-assisted laser desorption ionization time-of-flight mass spectroscopy; CCA, α -cyano-4-hydroxycinnamic acid; FRET, Förster resonance energy transfer; NCBI, National Center for Biotechnology Information; PDB, Protein Data Bank; KEGG, Kyoto Encyclopedia of Genes and Genomes; DMF, dimethylformamide.

■ REFERENCES

- (1) Hengge, R. (2009) Principles of c-di-GMP signalling in bacteria. *Nat. Rev. Microbiol.* 7, 263–273.
- (2) Schirmer, T., and Jenal, U. (2009) Structural and mechanistic determinants of c-di-GMP signalling. *Nat. Rev. Microbiol.* 7, 724–735.
- (3) Nakayama, S., Kelsey, I., Wang, J., Roelofs, K., Stefane, B., Luo, Y., Lee, V. T., and Sintim, H. O. (2011) Thiazole orange-induced c-di-GMP quadruplex formation facilitates a simple fluorescent detection of this ubiquitous biofilm regulating molecule. *J. Am. Chem. Soc.* 133, 4856–4864.
- (4) Wang, J., Zhou, J., Donaldson, G. P., Nakayama, S., Yan, L., Lam, Y. F., Lee, V. T., and Sintim, H. O. (2011) Conservative change to the phosphate moiety of cyclic diguanylic monophosphate remarkably affects its polymorphism and ability to bind DGC, PDE, and PilZ proteins. *J. Am. Chem. Soc.* 133, 9320–9330.
- (5) Luo, Y., Zhou, J., Watt, S. K., Lee, V. T., Dayie, T. K., and Sintim, H. O. (2012) Differential binding of 2'-biotinylated analogs of c-di-GMP with c-di-GMP riboswitches and binding proteins. *Mol. Biosyst.* 8, 772–778.
- (6) Chatterji, D., and Gopal, V. (1996) Fluorescence spectroscopy analysis of active and regulatory sites of RNA polymerase. *Methods Enzymol.* 274, 456–478.
- (7) Hiratsuka, T. (1982) New fluorescent analogs of cAMP and cGMP available as substrates for cyclic nucleotide phosphodiesterase. *J. Biol. Chem.* 257, 13354–13358.
- (8) Reddy, P. S., Raghavan, A., and Chatterji, D. (1995) Evidence for a ppGpp-binding site on *Escherichia coli* RNA polymerase: Proximity relationship with the rifampicin-binding domain. *Mol. Microbiol.* 15, 255–265.
- (9) Newton, M., Niewczas, I., Clark, J., and Bellamy, T. C. (2010) A real-time fluorescent assay of the purified nitric oxide receptor, guanylyl cyclase. *Anal. Biochem.* 402, 129–136.
- (10) Johnson, J. D., Walters, J. D., and Mills, J. S. (1987) A continuous fluorescence assay for cyclic nucleotide phosphodiesterase hydrolysis of cyclic GMP. *Anal. Biochem.* 162, 291–295.
- (11) Ren, J., and Goss, D. J. (1996) Synthesis of a fluorescent 7-methylguanosine analog and a fluorescence spectroscopic study of its reaction with wheatgerm cap binding proteins. *Nucleic Acids Res.* 24, 3629–3634.
- (12) Pisareva, V. P., Pisarev, A. V., Hellen, C. U. T., Rodnina, M. V., and Pestova, T. V. (2006) Kinetic analysis of interaction of eukaryotic release factor 3 with guanine nucleotides. *J. Biol. Chem.* 281, 40224–40235.
- (13) Spangler, C., Kaever, V., and Seifert, R. (2011) Interaction of the diguanylate cyclase YdeH of *Escherichia coli* with 2',(3')-substituted purine and pyrimidine nucleotides. *J. Pharmacol. Exp. Ther.* 336, 234–241.
- (14) Rensland, H., John, J., Linke, R., Simon, I., Schlichting, I., Wittinghofer, A., and Goody, R. S. (1995) Substrate and product structural requirements for binding of nucleotides to H-ras p21: The mechanism of discrimination between guanosine and adenosine nucleotides. *Biochemistry* 34, 593–599.
- (15) Lenzen, C., Cool, R. H., and Wittinghofer, A. (1995) Analysis of intrinsic and CDC25 stimulated guanine nucleotide exchange of p21ras-nucleotide complexes by fluorescence measurements. *Methods Enzymol.* 255, 95–109.
- (16) Stryer, L. (1978) Fluorescence energy transfer as a spectroscopic ruler. *Annu. Rev. Biochem.* 47, 819–846.
- (17) Kumar, K. P., and Chatterji, D. (1990) Resonance energy transfer study on the proximity relationship between the GTP binding site and the rifampicin binding site of *Escherichia coli* RNA polymerase. *Biochemistry* 29, 317–322.
- (18) Sullivan, S. M., Mishra, R., Neubig, R. R., and Maddock, J. R. (2000) Analysis of guanine nucleotide binding and exchange kinetics of the *Escherichia coli* GTPase Era. *J. Bacteriol.* 182, 3460–3466.
- (19) Chan, C., Paul, R., Samoray, D., Amiot, N. C., Giese, B., Jenal, U., and Schirmer, T. (2004) Structural basis of activity and allosteric control of diguanylate cyclase. *Proc. Natl. Acad. Sci. U.S.A.* 101, 17084–17089.

- (20) Arnold, K., Bordoli, L., Kopp, J., and Schwede, T. (2006) The SWISS-MODEL workspace: A web-based environment for protein structure homology modelling. *Bioinformatics* 22, 195–201.
- (21) Lasckowski, R. A., MacArthur, M. W., Moss, D. S., and Thornton, J. M. (1993) PROCHECK: A program to check the stereochemical quality of protein structures. *J. Appl. Crystallogr.* 26, 283–291.
- (22) Simm, R., Morr, M., Kader, A., Nimtz, M., and Römling, U. (2004) GGDEF and EAL domains inversely regulate cyclic di-GMP levels and transition from sessility to motility. *Mol. Microbiol.* 53, 1123–34.
- (23) Woodward, J. J., Iavarone, A. T., and Portnoy, D. A. (2010) c-di AMP secreted by intracellular *Listeria monocytogenes* activates a host type I interferon response. *Science* 328, 1703–1705.
- (24) Kamegaya, T., Kuroda, K., and Hayakawa, Y. (2011) Identification of a *Streptococcus pyogenes* SF370 gene involved in production of c-di-AMP. *Nagoya J. Med. Sci.* 73, 49–57.
- (25) Christen, B., Christen, M., Paul, R., Schmid, F., Folcher, M., Jenoe, P., Meuwly, M., and Jenal, U. (2006) Structural basis of activity and allosteric control of diguanylate cyclase. *J. Biol. Chem.* 281, 32015–32024.
- (26) Wassmann, P., Chan, C., Paul, R., Beck, A., Heerklotz, H., Jenal, U., and Schirmer, T. (2007) Structure of BeF₃[−]-modified response regulator PleD: Implications for diguanylate cyclase activation, catalysis, and feedback inhibition. *Structure* 15, 915–927.
- (27) Ching, S. M., Tan, W. J., Chua, K. L., and Lam, Y. (2010) Synthesis of cyclic dinucleotidic acids as potential inhibitors targeting diguanylate cyclase. *Bioorg. Med. Chem.* 18, 6657–6665.
- (28) Bharati, B. K., Sharma, I. M., Kasetty, S., Kumar, M., Mukherjee, R., and Chatterji, D. (2012) A full length bifunctional protein involved in c-di-GMP turnover is required for long term survival under nutrient starvation in *Mycobacterium smegmatis*. *Microbiology* 158, 1415–1427.
- (29) Rao, F., Yang, Y., Qi, Y., and Liang, Z. X. (2008) Catalytic mechanism of cyclic di-GMP specific phosphodiesterase: A study of the EAL domain-containing RocR from *Pseudomonas aeruginosa*. *J. Bacteriol.* 190, 3622–3631.
- (30) Amikam, D., and Galperin, M. Y. (2006) PilZ domain is part of the bacterial c-di-GMP binding protein. *Bioinformatics* 22, 3–6.
- (31) Ryjenkov, D. A., Simm, R., Römling, U., and Gomelsky, M. (2006) The PilZ domain is a receptor for the second messenger c-di-GMP. *J. Biol. Chem.* 281, 30310–30314.
- (32) Pratt, J. T., Tamayo, R., Tischler, A. D., and Camilli, A. (2007) PilZ domain proteins bind cyclic diguanylate and regulate diverse processes in *Vibrio cholera*. *J. Biol. Chem.* 282, 12860–12870.
- (33) Benach, J., Swaminathan, S. S., Tamayo, R., Handelman, S. K., Folta-Stogniew, E., Ramos, J. E., Forouhar, F., Neely, H., Seetharaman, J., Camilli, A., and Hunt, J. F. (2007) The structural basis of cyclic diguanylate signal transduction by PilZ domains. *EMBO J.* 26, 5153–5166.
- (34) Friedman, M. L., Schlueter, K. T., Kirley, T. L., and Halsall, H. B. (1985) Fluorescence quenching of human orosomucoid. Accessibility to drugs and small quenching agents. *Biochem. J.* 232, 863–867.
- (35) Tamayo, R., Tischler, A. D., and Camilli, A. (2005) The EAL domain protein VieA is a cyclic diguanylate phosphodiesterase. *J. Biol. Chem.* 280, 33324–33330.
- (36) Christen, M., Christen, B., Folcher, M., Schauerte, A., and Jenal, U. (2005) Identification and characterization of a cyclic di-GMP-specific phosphodiesterase and its allosteric control by GTP. *J. Biol. Chem.* 280, 30829–30837.